Impaired Light Adaptation of ON-Sustained Ganglion Cells in Early Diabetes Is Attributable to Diminished Response to Dopamine D4 Receptor Activation

Michael D. Flood, Andrea J. Wellington, and Erika D. Eggers

Departments of Physiology and Biomedical Engineering, University of Arizona, Tucson, Arizona, United States

Correspondence: Erika Eggers, Departments of Physiology and Biomedical Engineering, P.O. Box 245051, University of Arizona, Tucson, AZ 85724, USA; eeggers@arizona.edu.

Purpose. Retinal neuronal signaling is disrupted early in diabetes, before the onset of the vascular pathologies associated with diabetic retinopathy. There is also growing evidence that retinal dopamine, a neuromodulator that mediates light adaptation, is reduced in early diabetes. Previously, we have shown that after 6 weeks of diabetes, light adaptation is impaired in ON-sustained (ON-s) ganglion cells in the mouse retina. The purpose of this study was to determine whether changes in the response to dopamine receptor activation contribute to this dysfunction.

Methods. Single-cell retinal patch-clamp recordings from the mouse retina were used to determine how activating dopamine type D4 receptors (D4Rs) changes the light-evoked and spontaneous excitatory inputs to ON-s ganglion cells, in both control and 6-week diabetic (STZ-injected) animals. Fluorescence *in situ* hybridization was also used to assess whether D4R expression was affected by diabetes.

Results. D4R activation decreased light-evoked and spontaneous inputs to ON-s ganglion cells in control and diabetic retinas. However, D4R activation caused a smaller reduction in light-evoked excitatory inputs to ON-s ganglion cells in diabetic retinas compared to controls. This impaired D4R signaling is not attributable to a decline in D4R expression, as there was no change in D4R mRNA density in the diabetic retinas.

Conclusions. These results suggest that the cellular response to dopamine signaling is disrupted in early diabetes and may be amenable to chronic dopamine supplementation therapy.

Keywords: retina, ganglion cell, dopamine, light adaptation, diabetes

By 2050, it is estimated that 16 million Americans will be afflicted with diabetic retinopathy, with one-fifth having vision-threatening complications.[1] This presents a major challenge to health care in the coming decades. Current clinical interventions largely target the vascular changes that occur with the onset of diabetic retinopathy. However, it has become increasingly clear that diabetes affects the neural retina long before functional changes in the retinal vasculature can be observed. Studies using electroretinograms (ERGs) have identified measurable changes in retinal activity in human diabetic patients[2–4] who do not exhibit any clinical signs of retinopathy. Similar deficits in ERGs are detected in rodent models of early diabetes,[5] and single-cell studies in these models have further identified electrical dysfunction at the single-cell level.[6–9] Interestingly, multifocal ERG studies have demonstrated that these changes in electrical activity develop asymmetrically across the retina and that localized sites of disrupted neural activity precede and predict the sites of future vascular pathology.[2,10–12] Thus, it is highly likely that the neuronal changes in retinal activity that are occurring early on in diabetes are involved in the progression of diabetic retinopathy.

In a recent study, we showed that 6 weeks of diabetes reduces the ability of ON-sustained (ON-s) ganglion cells to adapt to increased background light.[13] The retina's ability to adapt to background light over a wide range of lighting conditions, a process known as light adaptation, is crucial to normal visual function.[14–16] In the healthy retina, light adaptation is mediated in part by dopamine release from dopaminergic amacrine cells.[15,17,18] Dopamine functions in a paracrine manner by binding to D1, D2, and D4 receptors (R) located on retinal neurons.[19–24] There is growing evidence that dopaminergic signaling is affected in early diabetes[25–28] and could contribute to the observed changes in light adaptation. However, it is unknown whether this disruption is attributable to changes in downstream targets of dopamine, diminished release of dopamine by dopaminergic amacrine cells, or both.

Here, we sought to determine whether retinal responses to dopamine are affected in early diabetes. This was examined in ON-s ganglion cells that have previously shown impaired light adaptation in diabetes.[13] The modulation of light-evoked and spontaneous excitatory currents by a D4R agonist in control and diabetic cells was measured to identify any impairment in dopaminergic signaling. In addition, the levels of D4R mRNA in control and diabetic retinas were quantified to assess whether changes in receptor expression were responsible for dopaminergic dysfunction.

METHODS

Animals

Animal protocols followed the ARVO Statement for the Use of Animals in Ophthalmic and Visual Research and were approved by the University of Arizona Institutional Animal Care and Use Committee. C57BL/6J male mice (Jackson Laboratories, Bar Harbor, ME, USA) were housed in the University of Arizona animal facility and given the National Institutes of Health–31 rodent diet food and water ad libitum. Five-week-old mice were fasted for 4 hours and injected intraperitoneally with either streptozotocin (STZ; 75 mg/kg body weight) dissolved in 0.01 M (pH 4.5) citrate buffer or citrate buffer vehicle for 3 consecutive days.[6] Six weeks after injections, fasted (4 hours) blood glucose was measured (OneTouch UltraMini; LifeScan, Milpitas, CA, USA). STZ-injected animals with blood glucose ≤ 200 mg/dL and control animals with blood glucose ≥ 200 mg/dL were eliminated from the study. Fasting blood glucose was 135 ± 12 mg/dL (control, $n = 12$ mice) or 376 ± 28 mg/dL (STZ, $n = 13$ mice; $P < 0.001$), and body weights were 23.1 ± 2.0 g (control) and 20.9 ± 0.7 g (STZ).

Whole-Cell Recordings

As previously described,[29] six weeks after injections, mice were euthanized using carbon dioxide, the eyes were enucleated, and the cornea and lens were removed to form an eyecup. The eyecup was incubated in cold extracellular solution with hyaluronidase (800 U/mL, 20 minutes) and washed with cold extracellular solution, and the retina was removed. For slice preparations, the retina was trimmed into a rectangle, mounted onto nitrocellulose filter paper (0.45-µm; Millipore, Billerica, MA, USA), transferred to a hand chopper and sliced (250 µm), rotated 90°, and mounted onto glass coverslips using vacuum grease. Whole mounts were prepared according to previous methods.[30,31] The retina was cut into four equal quadrants and mounted photoreceptor side down onto a trimmed cell culture insert (1 mm height; Millipore Sigma, Burlington, MA, USA). All dissections and light response recording procedures were performed under infrared illumination to preserve the light sensitivity.

Extracellular solution was bubbled with a mixture of 95% O_2–5% CO_2 (pH to ~7.4) and contained (in mM) the following: 125.00 NaCl, 2.50 KCl, 1.00 $MgCl_2$, 1.25 NaH_2PO_4, 20.00 glucose, 26.00 $NaHCO_3$, and 2.00 $CaCl_2$. Intracellular solution in the recording pipette contained (in mM) the following: 120.00 CsOH, 120.00 gluconic acid, 1.00 $MgCl_2$, 10.00 HEPES, 10.00 EGTA, 10.00 tetraethylammonium-Cl, 10.00 phosphocreatine-Na_2, 4.00 Mg-ATP, 0.50 Na-GTP, and 0.1% sulforhodamine-B dissolved in water (pH 7.2 with CsOH). To selectively activate D4Rs, the D4R agonist PD-168077-maleate (PD, 500 nM; solubilized in DMSO Waltham, Massachusetts, USA) was diluted in extracellular solution and applied to the recording bath by a gravity-driven superfusion system (Cell Microcontrols, Norfolk, VA, USA; ~1 mL/min). The perfusate had a final DMSO concentration of less than 0.0025%. Chemicals were purchased from Sigma-Aldrich (St. Louis, MO, USA) unless otherwise indicated.

Responses were recorded in a control dark-adapted state, agonist was applied for 5 minutes, and then responses were recorded in the continuous presence of agonist. Retinal slices on glass coverslips or whole-mount preps were placed in a custom chamber and heated to 32° (TC-324 temperature controller with SH-27B inline heater; Warner Instruments, Hamden, CT, USA). Whole-cell voltage-clamp recordings of light-evoked (L-) and spontaneous (s) excitatory postsynaptic currents (EPSCs) were made from ON-s ganglion cells voltage clamped at –60 mV, the reversal potential for Cl⁻ currents. Series resistance was uncompensated. Electrodes with resistances of 3 to 7 MΩ were pulled (borosilicate glass; World Precision Instruments, Sarasota, FL, USA) using a P97 Flaming/Brown puller (Sutter Instruments, Novato, CA, USA). Calculated liquid junction potentials of 20 mV (Clampex; Molecular Devices, Sunnyvale, CA, USA), were corrected before recording. Recordings were sampled at 10 kHz, filtered at 6 kHz (Bessel filter, Multi-Clamp 700B amplifier; Molecular Devices), and digitized with a Digidata 1140 and Clampex software (Molecular Devices).

During whole-cell recordings, cells were passively filled with sulforhodamine-B included in the intracellular solution. ON-s ganglion cells were targeted by their large soma size (>15 µM diameter).[32] Similar to a previous report,[13] confirmation of ganglion cell morphology and presence of an axon was done at the end of each recording using an Intensilight fluorescence lamp and Digitalsight camera controlled by Elements software (Nikon Instruments, Tokyo, Japan). Ganglion cells were further characterized by their light-evoked EPSC resulting from a 500-ms duration $9.5 \cdot 10^5$ photons·µm^{-2}·s^{-1} flash of light. They were classified as ON-sustained if a light-evoked EPSC coincided with the onset of light, did not return to baseline until after light offset, and did not possess a distinct OFF response as well.

Light Stimuli

Full-field light stimuli were evoked with a light-emitting diode (LED; HLMP-3950, λpeak = 525 nm; Agilent, Palo Alto, CA, USA) that was calibrated with an S471 optometer (Gamma Scientific, San Diego, CA, USA) and projected through the camera port of the microscope via a 4× objective. Stimuli frequency (1/30 seconds), intensities, and duration (30 ms) were controlled by varying the current through the LED. The stimulus intensities were chosen to cover the mesopic range of light intensities (9.5, 95.0, 950.0, $9.5 \cdot 10^3$, $9.5 \cdot 10^4$, and $9.5 \cdot 10^5$ photons·µm^{-2}·s^{-1}). These intensities were calculated to be equivalent to 4.75, 47.50, 475.00, $4.75 \cdot 10^3$, $4.75 \cdot 10^4$, and $4.75 \cdot 10^5$ R*·rod^{-1}·s^{-1}, respectively.[33]

Data Analysis and Statistics

2 to 4 L-EPSC traces for each condition were averaged using Clampfit (Molecular Devices). The peak amplitude, charge transfer (Q), time to peak, and decay to 37% of the peak (D37) were determined. For each cell, the timing of the longest duration response (from the beginning to return to baseline, typically 1-2 seconds) was measured, and these times were used to calculate Q for all responses from that cell. Time to peak and D37 were calculated as the temporal differences between response peak amplitude and stimulus onset or decline to 37% of peak amplitude, respectively. L-EPSC data from each cell were normalized to the response recorded for that cell at the maximum intensity in dark-adapted conditions. If there was no response for a given light intensity after averaging, the peak amplitude was recorded as 0, and it was excluded from analysis of response kinetics. Comparisons between experimental conditions and luminance intensities were made with two-way ANOVA tests using the

Student–Newman–Keuls (SNK) method for pairwise comparisons in SigmaPlot (Systat Software, San Jose, CA, USA). If any data were shown to have a nonnormal distribution or unequal variance, tests were repeated on the $\log_{10}$ values (or square root values for peak amplitudes) of data.

Spontaneous events were analyzed in the baseline after a light response up to 1 second before the subsequent light stimulus. Events were identified via the MATLAB code and methodology outlined in Andor-Ardo et al.[34] Frequency, amplitude, interevent interval (IEI), and decay τ (single exponent fit) for identified sEPSCs were calculated using custom-written MATLAB (MathWorks, Natick, MA, USA) scripts. Effects of treatment on sEPSCs were analyzed at the single cell level with Kolmogorov–Smirnov (K-S) tests. To allow for visualization of the impact of the D4R agonist across cells, amplitude, decay τ, and IEI cumulative distributions were normalized along the x-axis to the maximum value recorded for each cell. D4R agonist effects on average sEPSC parameters were normalized to the dark-adapted state for each cell and analyzed before and after agonist with paired *t*-tests and between different groups of cells (control versus diabetic) with unpaired *t*-tests. Cells were included in the analysis if they had 10 or more spontaneous events per treatment condition. Differences were considered significant when $P \leq 0.05$ and data are reported as means $\pm$ 95% confidence intervals.

mRNA Imaging and Analysis

Mouse eyecups were prepared as described above. Retinas were fixed in the eyecup (24 hours, room temperature), rinsed in PBS, dissected out of the eyecup, stored in 70% EtOH at 4°C (<7 days), embedded in paraffin, sliced at 5 µm onto Fisher Superfrost slides (#12-550-17; Fisher, Waltham, Massachusetts, USA) and air-dried overnight (room temperature). Slides were baked (60°C, 1 hour), dewaxed, treated with alcohol, baked again (30 minutes, 60°C), and incubated with ER 2 (95°C, 5 minutes) and protease (1:15 dilution, 15 minutes). Slides were run on a Leica BOND automatic slide processor (Leica Biosystems, Wetzlar, Germany) using the RNAscope LS Multiplex Fluorescent Reagent Kit (#322800; ACD, USA) and the RNAscope probe 2.5LS Mm-Drd4 (#418178; ACD) following the manufacturer's instructions. Positive (Mm-Polr2a, #320888; ACD) and negative (against the bacteria-specific transcript DapB, #320878; ACD) control probes were used on control retina slices and run alongside experimental retinal slices.

Slides were imaged on a Zeiss LSM 880 inverted confocal microscope (Carl Zeiss Microscopy, Oberkochen, Germany) with a 40× objective (Plan-Apochromat 40×/1.3 oil) and a Z-stack step of 0.38 µm. Drd4 mRNA signal was detected using the 488-nm laser at 7% intensity with pinhole set at 1 Airy unit (AU) and was collected between 498 and 553 nm. DAPI nuclear staining was detected with the 405-nm laser at 0.5% intensity with pinhole at 1 AU and was collected between 410 and 480 nm. The laser detection intensity was set such that minimal signal was detected on negative control slides.

Images were analyzed with ImageJ (National Institutes of Health, Bethesda, MD, USA). Maximum intensity projections of five slices from each Z-stack were analyzed. After subtracting background, regions of interest (ROIs) were drawn around each retinal layer on the despeckled, thresholded image (threshold set at 20% of maximum intensity of Drd4 in the inner nuclear layer). Analyze Particles was used to select and measure Drd4-positive mRNA particles in

each layer. The results were analyzed by a custom MATLAB program. Each retina measurement reported is from two independently run slices, which were averaged.

Results

D4R Activation Decreases the Magnitude of L-EPSCs in Control and Diabetic ON-s Ganglion Cells

To assess whether D4R modulation of ON-s ganglion cell L-EPSCs was affected after 6 weeks of diabetes, light responses were first recorded in dark-adapted ON-s ganglion cells from control mice (control, Fig. 1A) before and after application of a D4R agonist (PD, 500 nM). To adjust for any differences in connectivity or responsivity between retinas, normalized values were compared for all analyses (see Methods). D4R activation significantly decreased peak amplitude (Fig. 1B, Table) and charge transfer (Q, Fig. 1C) at all except the dimmest light intensity (SNK, $P < 0.05$). D4R activation also significantly delayed time to peak values (Fig. 1D), mainly due to differences at 95 photons·µm^{-2}·s^{-1} (SNK, $P = 0.025$). No change in D37 values was recorded (Fig. 1E).

D4R activation also modulated ON-s ganglion cells from diabetic mice (Fig. 2A). D4R activation significantly decreased peak amplitude (Fig. 2B, Table) with a pairwise difference at 950 photons·µm^{-2}·s^{-1} (SNK, $P < 0.05$) and significantly decreased Q (Fig. 2C) with specific differences at 950 and 9.5·10^4 photons·µm^{-2}·s^{-1} (SNK, $P < 0.05$). No difference was found for time to peak (Fig. 2D) or D37 (Fig. 2E) values. These findings suggest that even after 6 weeks of diabetes, activation of D4Rs significantly diminishes ON-s ganglion cell L-EPSCs and can continue to contribute to light adaptation.

D4R Modulation Is Reduced in Diabetic ON-s Ganglion Cells

To assess whether D4R activation was equivalent in control and diabetic ganglion cells, the values from the D4R agonist responses in Figures 1 and 2 were compared (Fig. 3). These values are normalized to the response to maximum light intensity in the dark-adapted retina, so if one group has larger values, this shows a decreased effect of the D4R agonist. Peak amplitude values were significantly higher in diabetic than control cells (Fig. 3A, Table), with specific differences at 9.5·10^5 photons·µm^{-2}·s^{-1} and 9.5·10^6 photons·µm^{-2}·s^{-1} (SNK $P < 0.05$). Q values were also significantly larger in diabetic than control cells (Fig. 3B), with a significant pairwise difference at 9.5·10^5 photons·µm^{-2}·s^{-1} (SNK, $P = 0.011$). No significant difference was found between the two groups in time to peak (Fig. 3C) or D37 (Fig. 3D). These data suggest that D4R activation has a smaller effect on L-EPSCs from diabetic ON-s ganglion cells.

Presynaptic Effects of D4R Activation on ON-s Ganglion Cell sEPSCs Remain Unperturbed After 6 Weeks of Diabetes

We previously showed that D4R activation decreases sEPSC frequency and amplitude in ON-s ganglion cells.[31] This suggests that D4R activation reduces ON bipolar cell release, shown by frequency reduction, and possibly causes postsynaptic changes in ON-s ganglion cells, shown by
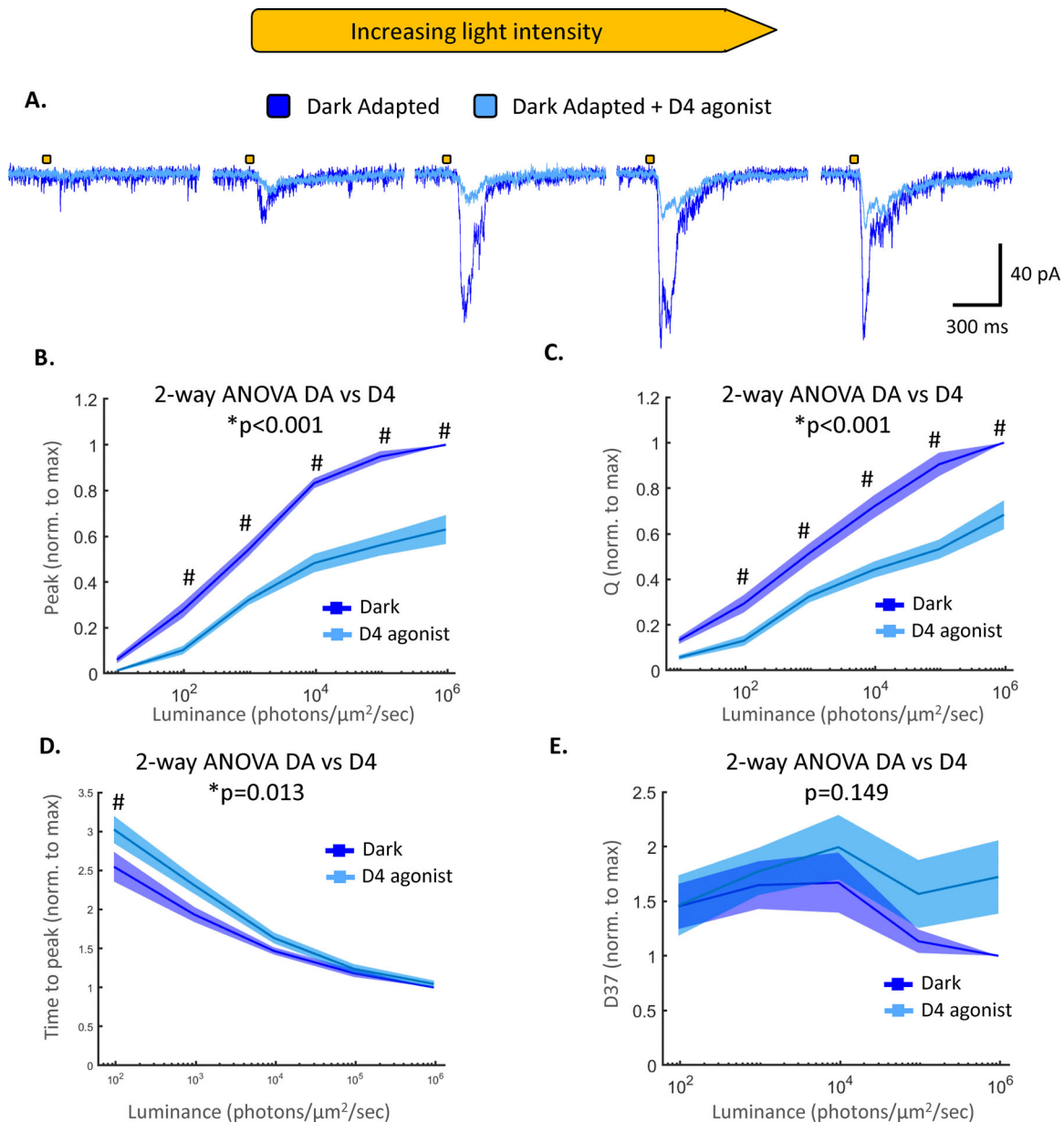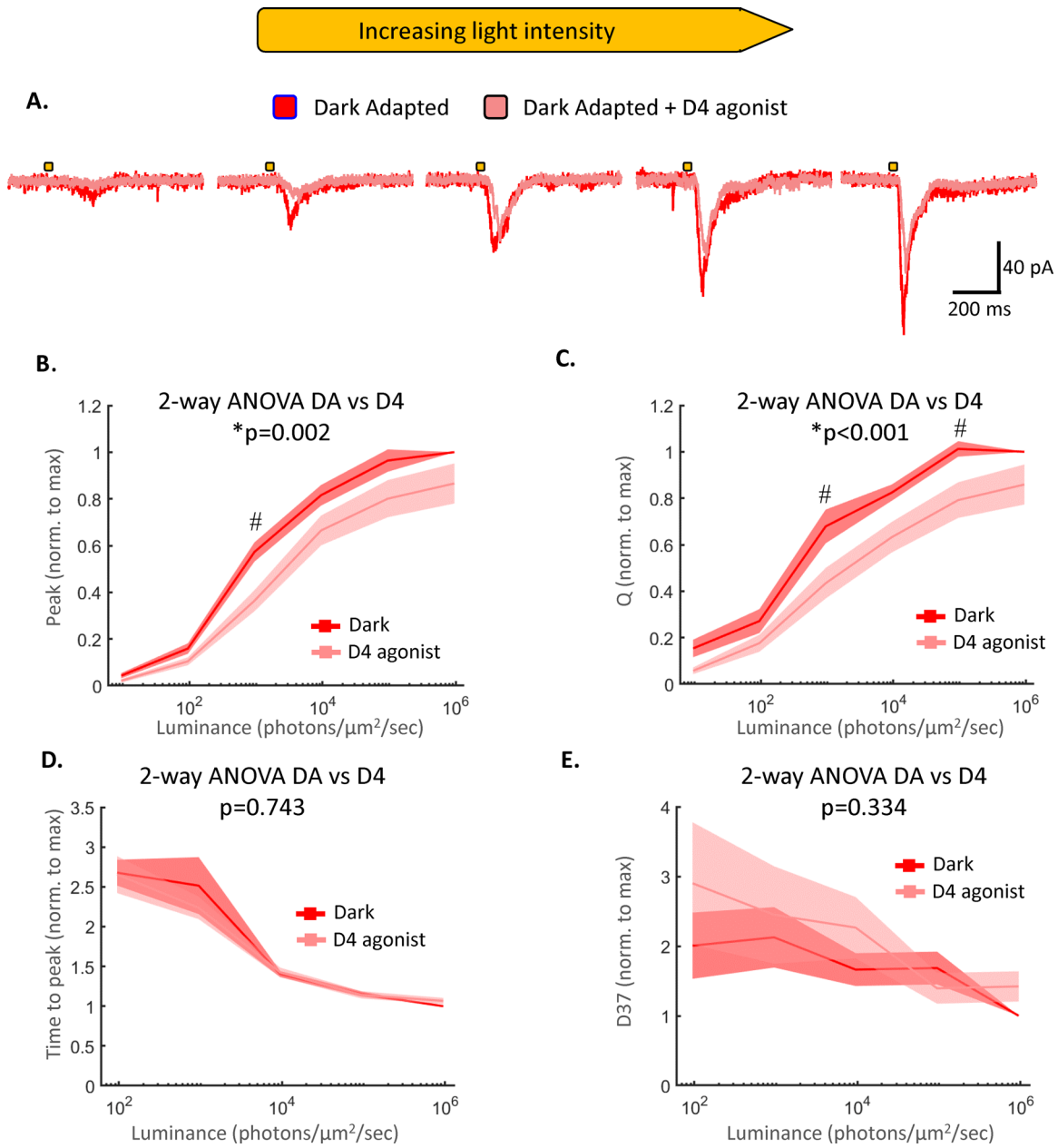
FIGURE 1. D4R activation decreases the magnitude and increases the times to peak of L-EPSCs in control ON-s ganglion cells. (**A**) Example L-EPSC traces from the same cell at increasing light intensities before (*dark blue*) and after (*light blue*) application of the D4R agonist PD-168077 maleate (500 nM). The *gold bars* represent 30-ms light stimuli. (**B–E**) Comparison of average peak amplitude (**B**), Q (**C**), time to peak (**D**), and D37 (**E**) between dark-adapted and D4R-agonized conditions. All values are normalized on a cell-by-cell basis to the response recorded at the maximum intensity in dark-adapted conditions. Main-effects p values for 2-way ANOVAs between treatment conditions are shown. *Significantly different main effect between dark-adapted and agonist-treated states. #Significantly different pairwise comparison between dark-adapted and D4R activated states at specific light intensity. $n = 13$ cells from eight animals.

amplitude reduction. To determine if the impaired D4R function seen in diabetic L-EPSCs was attributed to changes in ON-s ganglion cells or presynaptic circuits, sEPSCs were analyzed from the same control and diabetic cells from Figures 1 and 2 (see Methods). In control ON-s ganglion cells, D4R activation decreased average sEPSC amplitude, decay τ, and frequency (Figs. 4A, 4B). When the distributions of sEPSC values in individual cells were compared (Fig. 4C), D4R activation significantly shifted sEPSC distributions toward smaller amplitudes (7/8 cells; K-S, $p < 0.05$), shorter decay τs (6/8 cells; K-S, $p < 0.05$),

and longer interevent intervals (6/8 cells; K-S, $P < 0.05$). This suggests that for most control cells, D4R activation results in presynaptic changes to ON bipolar cell release and possibly to postsynaptic changes in ON-s ganglion cells.

For diabetic ganglion cells, D4R activation significantly decreased average sEPSC amplitude and frequency but not decay τ (Figs. 5A, 5B). When the distributions of sEPSC values in individual cells were compared (Fig. 5C), D4R activation significantly shifted sEPSC distributions toward smaller amplitudes (7/9 cells; K-S, $p < 0.05$), shorter decay

FIGURE 2. D4R activation decreases the magnitude but not kinetics of L-EPSCs in diabetic ON-s ganglion cells. (**A**) Example L-EPSC traces from the same cell at increasing light intensities before (*dark red*) and after (*light red*) application of the D4R agonist PD-168077 maleate (500 nM). The *gold bars* represent 30-ms light stimuli. (**B–E**) Comparison of average peak amplitude (**B**), Q (**C**), time to peak (**D**), and D37 (**E**) between dark-adapted and D4R-agonized conditions. All values are normalized on a cell-by-cell basis to the response recorded at the maximum intensity in dark-adapted conditions. Main-effects p values for 2-way ANOVAs between treatment conditions are shown. *Significantly different main effect between dark-adapted and agonist-treated states. #Significantly different pairwise comparison between dark-adapted and D4R activated states at specific light intensity. n = 12 cells from 10 animals.

τs (6/9 cells; K-S, $P < 0.05$), and longer interevent intervals (7/9 cells; K-S, $P < 0.05$). Thus, sEPSCs from diabetic ON-s ganglion cells responded to a D4R agonist in a similar fashion as controls.

To compare the magnitude of D4R-induced sEPSC changes in control and diabetic ganglion cells, average sEPSC values after D4R activation for each cell were normalized to those recorded before D4R activation. There were no significant differences in the effects of D4R activation on sEPSC amplitude or frequency (Figs. 6A, 6C) between control

and diabetic ON-s ganglion cells, suggesting similar degrees of modulation. Although a difference between control and diabetic cells in decay τ modulation might have been expected since D4R activation significantly reduced decay τs in control but not diabetic ganglion cells, there was no significant difference (Fig. 6B). Overall, these results suggest that D4R activation still affects the output of ON cone bipolar cells to ON-s ganglion cells in diabetic retinas, but its postsynaptic actions on ON-s ganglion cells may or may not be impaired.

Table. Statistics for Comparisons of Values from Control and Diabetic L-EPSCs Before (DA) and After (D4R) the Addition of the D4R Agonist PD

| Mouse	Comparison	Measurement	*P* Value (Two-Way ANOVA)
Control	DA vs. D4R	Peak amplitude	<0.001*
Control	DA vs. D4R	Q	<0.001*
Control	DA vs. D4R	Time to peak	0.013*
Control	DA vs. D4R	D37	0.149
Diabetic	DA vs. D4R	Peak amplitude	0.002*
Diabetic	DA vs. D4R	Q	<0.001*
Diabetic	DA vs. D4R	Time to peak	0.743
Diabetic	DA vs. D4R	D37	0.334
Control vs. diabetic	D4R vs. D4R	Peak amplitude	0.003*
Control vs. diabetic	D4R vs. D4R	Q	0.002*
Control vs. diabetic	D4R vs. D4R	Time to peak	0.138
Control vs. diabetic	D4R vs. D4R	D37	0.328

* Indicates significance.
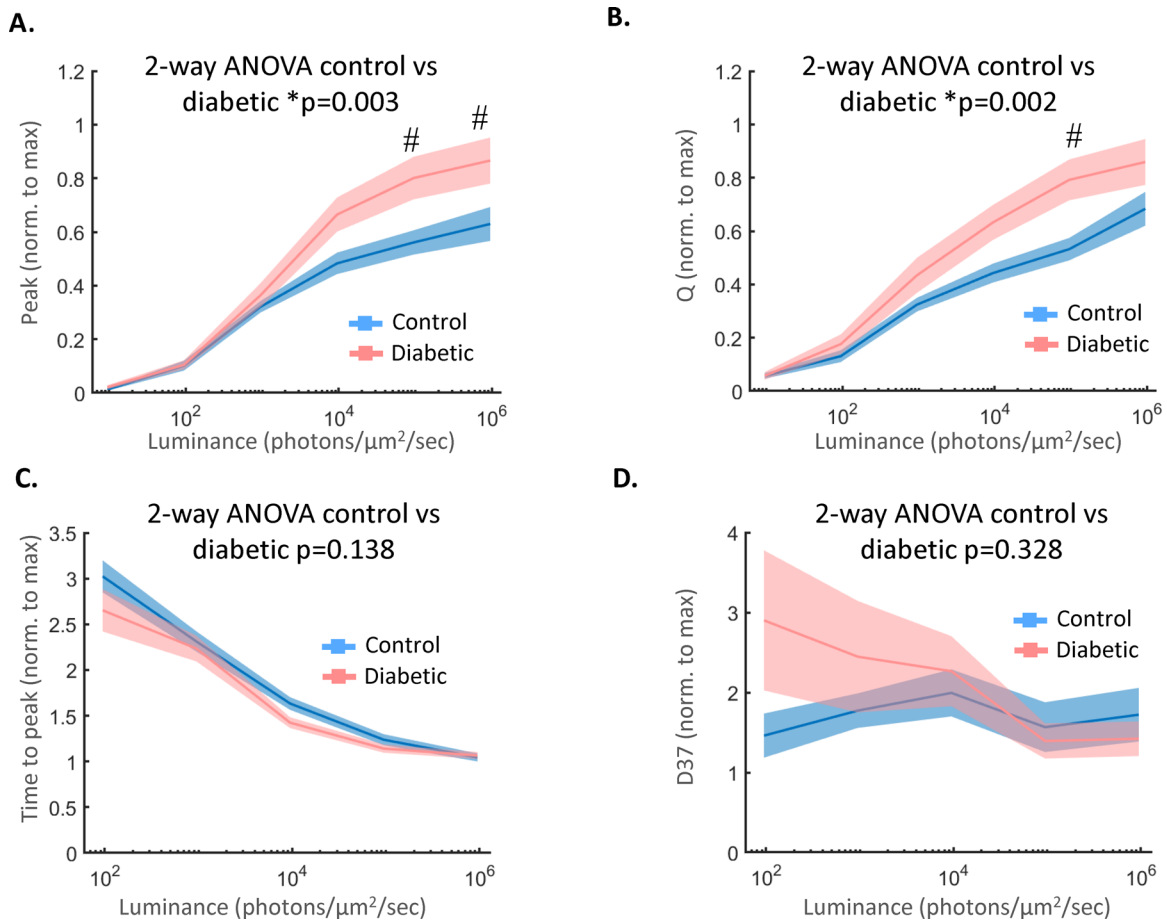
Figure 3. D4R activation causes larger decreases in L-EPSCs from control ON-s ganglion cells. **(A–D)** Comparison of normalized L-EPSC peak amplitude **(A)**, Q **(B)**, time to peak **(C)**, and D37 **(D)** values between control and diabetic cells after D4R activation. D4R activation reduced L-EPSC Q and peak amplitude to a greater degree in control ON-s ganglion cells than diabetic ones. *p* values for 2-way ANOVAs between conditions are shown. *Significantly different main effect between control and diabetic groups. #Significantly different pairwise comparison between control and diabetic groups at a specific light intensity. Values shown here are the same as the D4R-activated values from Figures 1 and 2.

A.
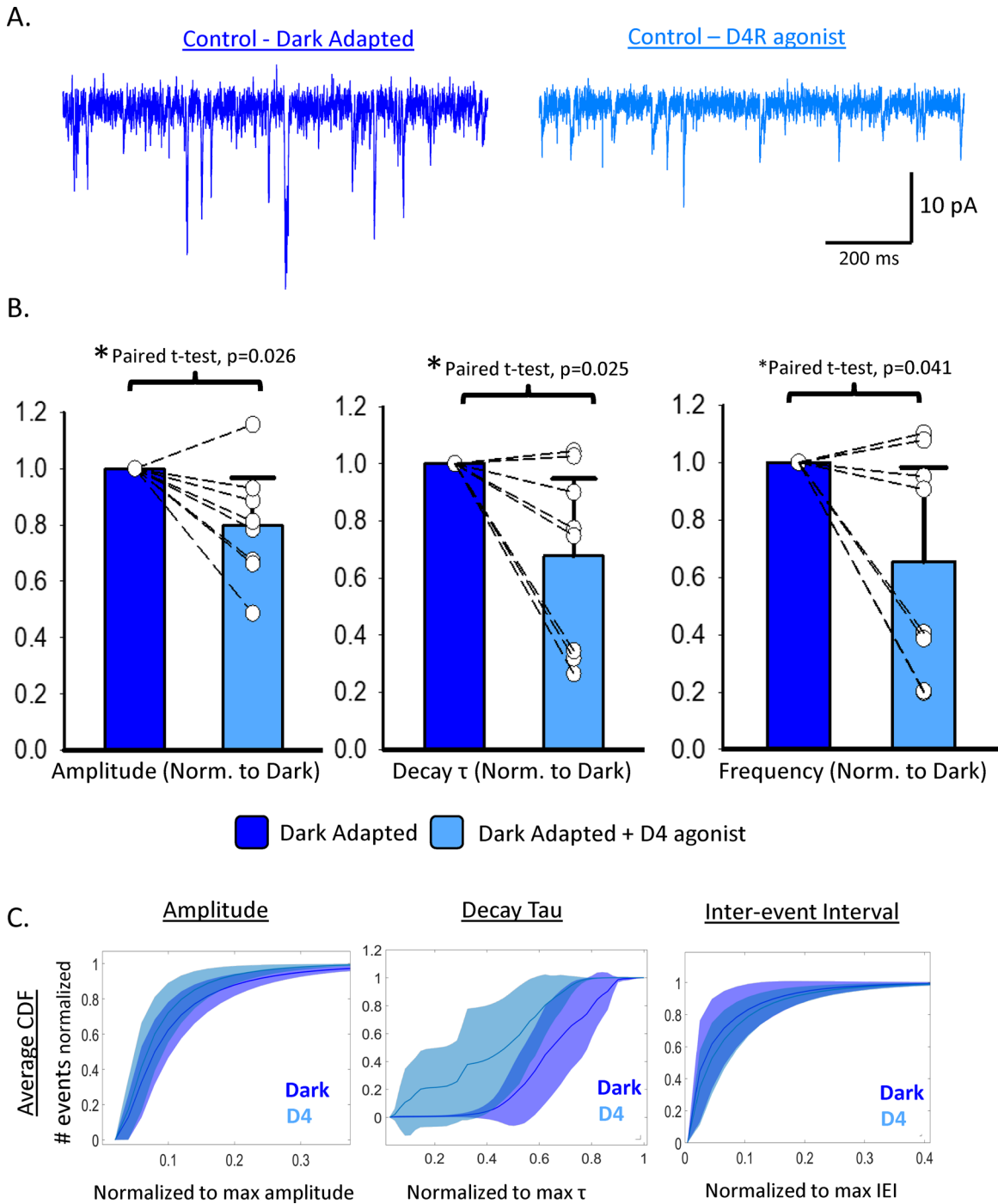
FIGURE 4. D4R activation decreases the amplitude, decay τ, and frequency of sEPSCs in control ON-s ganglion cells. (**A**) Example sEPSC traces from the same cell before (*dark blue, left*) and after (*blue, right*) application of the D4R agonist PD-168077 maleate (500 nM). (**B**) Average amplitude (*left*), decay τ (*middle*), and frequency (*right*) values of sEPSCs before (*dark blue*) and after (*light blue*) D4R activation, normalized to the dark-adapted values. Average values for individual cells are plotted as *white circles*. *Error bars* indicate average values + 95% confidence interval. (**C**) Normalized cumulative histograms (cumulative distribution function [CDF]) for sEPSC amplitudes (*left*), decay τs (*middle*), and interevent intervals (*right*). Individual CDFs were averaged for dark-adapted (*dark blue*) and D4R-activated (*light blue*) conditions. For each CDF, the y-axis was normalized to the total number of events recorded for each condition (either dark adapted or D4R activated), while the x-axis was normalized to the maximum value recorded on a cell-by-cell basis. Shaded areas represent 95% confidence intervals. $n = 8$ cells from five animals for all panels.
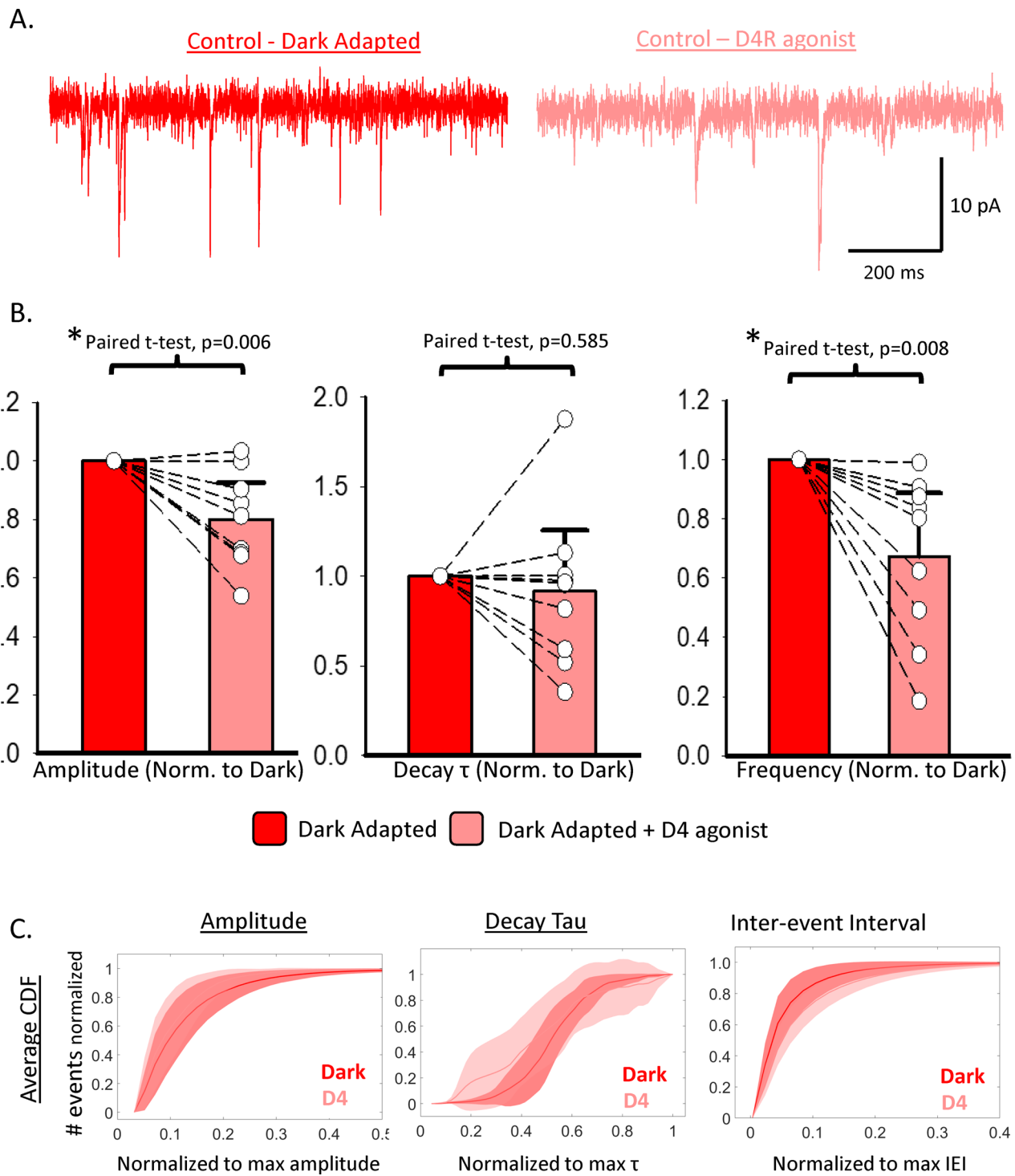
FIGURE 5. D4R activation decreases the amplitude and frequency of sEPSCs in diabetic ON-s ganglion cells. (**A**) Example sEPSC traces from the same cell before (*dark red, left*) and after (*light red, right*) application of the D4R agonist PD-168077 maleate (500 nM). (**B**) Average amplitude (*left*), decay τ (*middle*), and frequency (*right*) values of sEPSCs before (*red*) and after (*light red*) D4R activation, normalized to the dark-adapted values. Average values for individual cells are plotted as *white circles*. *Error bars* indicate average values + 95% confidence interval. (**C**) Normalized cumulative histograms for sEPSC amplitudes (*left*), decay τs (*middle*), and interevent intervals (right). Individual CDFs were averaged for dark-adapted (*red*) and D4R-activated (*light red*) conditions. For each CDF, the y-axis was normalized to the total number of events recorded for each condition, while the x-axis was normalized to the maximum value recorded on a cell-by-cell basis. Shaded areas represent 95% confidence intervals. $n = 9$ cells from seven animals for all panels.
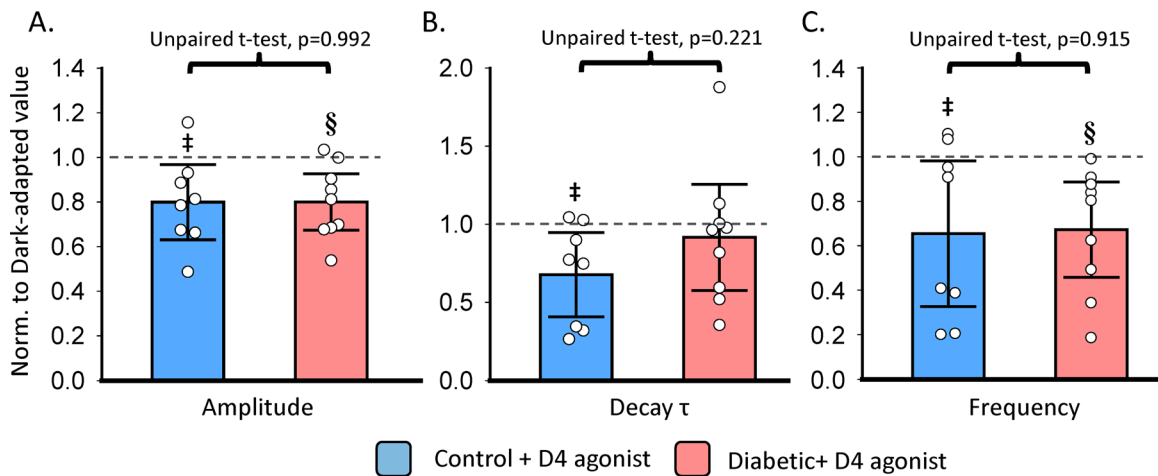
FIGURE 6. D4R activation decreases the amplitude and frequency of sEPSCs in control and diabetic ON-s ganglion cells by similar degrees. Average sEPSC amplitude (*left*), decay τ (*middle*), and frequency (*right*) in control (*light blue*) and diabetic (*light red*) ON-s ganglion cells after D4R activation. Data were normalized to dark-adapted values on a cell-by-cell basis before averaging, and individual data points are plotted as *white circles*. When directly comparing the degree to which D4R activation reduces these parameters in control and diabetic cells, no significant difference was found. *Error bars* represent 95% confidence intervals. Control $n = 8$ cells from five animals and diabetic $n = 9$ cells from seven animals. [‡,§]Significant difference between dark-adapted and D4R-treated values in control and diabetic ganglion cells, respectively. For all tests, significance level was set to $\alpha = 0.05$.

D4R mRNA Expression Is Unchanged After 6 Weeks of Diabetes

Changes in the response of light-evoked excitation to a D4R agonist could potentially be attributed to a decline in D4R expression. To asses this, D4R mRNA was fluorescently labeled in control and diabetic retinal slices using the RNAscope system (Figs. 7A–D). Both the number of D4R particles/ROI and the total D4R particle area/ROI were highest in the outer nuclear layer and photoreceptor inner segments (Fig. 7), as expected from previous results.[21–24] There were no significant differences in the number of D4R particles/ROI or in the D4R particle area/ROI between control and diabetic retinas (Fig. 7E; two-way repeated measures ANOVA-F; area $P = 0.724$, number $P = 0.798$). This shows that the reduction in D4R activity is not due to reductions in D4R expression.

DISCUSSION

Dopamine is a key neuromodulator for retinal light adaptation. Although there is evidence that dopaminergic signaling is disrupted early in diabetes in rodents,[25,28,35,36] no specific mechanisms of this disruption had been identified. Here we demonstrated reduced efficacy of a D4R agonist on retinal ganglion cell signaling in diabetic mice. Our data suggested that this was due to reduced dopamine sensitivity of outer retinal neurons and potentially the ON-s ganglion cells themselves. This impaired sensitivity is likely not due to a decline in D4R mRNA expression but could be caused by changes in the cellular machinery responsible for dopamine signal transduction.

D4R Activation Reduces Light-Evoked Excitation to ON-s Ganglion Cells in Both Control and Diabetic Retinas

D4R agonist reduced the size of L-EPSCs in ON-s ganglion cells in both control and diabetic animals. In the rodent retina, D4Rs are primarily expressed by photoreceptors (Fig. 7),[21,37,38] suggesting that D4Rs could reduce ganglion cell excitation by decreasing photoreceptor light sensitivity and/or decreasing photoreceptor output to bipolar cells. D4Rs on photoreceptors have been shown to reduce cAMP levels,[21,39–41] phosphorylation of phosducin,[42] and gap-junctional coupling between rod and cone photoreceptors in the mouse.[23] All of these mechanisms have been shown to reduce photoreceptor, especially rod, sensitivity to light.[43–46] Because there is evidence that D4R mRNA expression is unchanged[36] (Fig. 7) in diabetic retinas, it follows that D4R activation still had effects on L-EPSCs in both control and diabetic ON-s ganglion cells.

D4R-Mediated Reduction of Light-Evoked Currents Is Impaired in Diabetic Retinas

Total retinal dopamine content is decreased in rodent models of early diabetes.[25,28,35,36] We previously showed that light adaptation, which is in part due to retinal dopamine release, was also impaired in diabetic animals.[13] The reduced response of light-evoked currents to D4R agonist treatment in diabetic ON-s ganglion cells found here (Fig. 3) suggests that a diminished capacity for diabetic cells to respond to dopamine could contribute to reduced light adaptation. Since there was no decrease in D4R mRNA levels, this suggests that photoreceptors from diabetic retinas are deficient in the cellular machinery necessary to respond to dopaminergic signaling. Knocking out D4Rs in mouse photoreceptors reduces the expression of adenylyl cyclase,[27,40] the enzyme responsible for cAMP production, while application of a D4R agonist in wild-type animals increases adenylyl cyclase expression.[16] Interestingly, these results imply that the regular activation of D4Rs in photoreceptors is necessary for proper expression of the machinery that these cells require to respond to dopamine. Thus, since absolute retinal dopamine levels are decreased in early diabetes, a chronic hypoactivation of D4Rs could explain the impaired acute response to a D4R agonist.
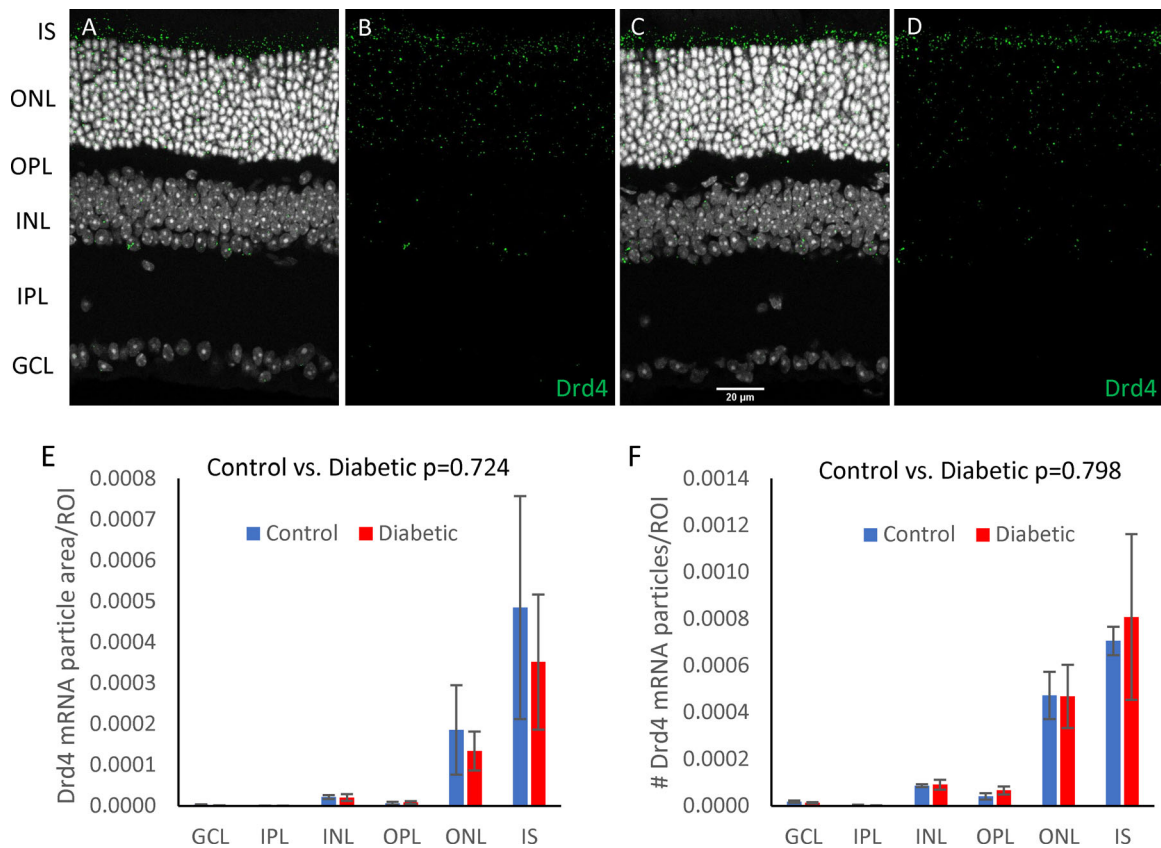
Figure 7. There was no difference in D4R mRNA levels between control and diabetic retinas. (**A–D**) Fluorescence *in situ* hybridization using the RNAscope system labeling D4R mRNA (*green*, Drd4) and DAPI (*white*) in control (**A**, **B**) and diabetic (**C**, **D**) retinal slices. (**E**, **F**) Drd4 mRNA particles were quantified by the area occupied by Drd4 particles per square micron of layer area (**E**) and as the number of Drd4 mRNA particles in each retinal layer shown, normalized to the area of that layer (**F**). No differences were found between control and diabetic retinas. $n = 4$ retinas from four mice for control, $n = 3$ retinas from three mice for diabetic. GCL, ganglion cell layer; INL, inner nuclear layer; IPL, inner plexiform layer; IS, photoreceptor inner segments; ONL, outer nuclear layer; OPL, outer plexiform layer.

D4R-Mediated Reduction in Tonic Glutamate Release by ON Cone Bipolar Cells Is Maintained in Diabetic Animals, but Postsynaptic Changes in ON-s Ganglion Cells May Be Impaired

In contrast to the reduced effect of D4Rs on light-evoked currents in ON-s ganglion cells from diabetic animals, there were no significant differences in D4R modulation of spontaneous current amplitudes, decay τs, and frequencies between control and diabetic groups. A decline in sEPSC frequency shows a decrease in tonic glutamate release by ON bipolar cells. This could potentially be due to a D4R-mediated reduction of photoreceptor calcium concentrations[47,48] that would cause sustained depolarization of ON bipolar cells. Sustained depolarization has been shown to cause activity-induced adaptation of bipolar cells[49] that would decrease tonic glutamate release onto ON-s ganglion cells. Because miniature EPSCs were not isolated in this study, it is possible that the observed changes in average sEPSC amplitude and decay τ could also be explained by the decrease in event frequency. A reduced rate of vesicle release by bipolar cells could reduce the probability of coordinated vesicle release, which in turn could affect amplitude and decay τ distributions. Alternatively, D4R expression has been reported in some populations of ganglion cells.[21,23,50] D2R/D4R agonists can modify potas-

sium, calcium, and voltage-gated sodium currents in dissociated rat ganglion cells,[51,52] so direct modulation of ON-s ganglion cell glutamate currents could cause sEPSC amplitude and decay τ changes. However, since there were no differences in D4R effects on sEPSCs between diabetic and control ON-s ganglion cells, any direct D4R effects on ON-s ganglion cells are not affected by diabetes.

Conclusions

Proper activity of retinal D4Rs is important for visual contrast sensitivity,[16,53] and contrast sensitivity deficits in diabetic mice[36] can be acutely resolved via injection of a D4R agonist. Given these results, as well as the findings reported here, it seems likely that a deficiency in dopaminergic signaling at least in part underlies reports of impaired contrast sensitivity in diabetic human populations that lack any clinical presentation of diabetic retinopathy.[54–57] In addition, there is growing evidence for D4Rs playing an important role in the circadian control of retinal metabolism,[27,58–60] as well as evidence for the disruption of these retinal circadian rhythms in early diabetes.[25,61–63] If this early impairment in dopaminergic signaling is the cause for dysregulated retinal metabolism, it could serve as a direct link between the visual deficits associated with early diabetes and the progression of this disease toward the more severe symptomology

of diabetic retinopathy. This would support using dopamine restorative therapies[64] as an early intervention in diabetic models and patient populations to prevent the serious retinal complications that arise upon disease progression.

References

1. Shukla UV, Tripathy K. Diabetic retinopathy. In: *StatPearls.* Treasure Island, FL: StatPearls Publishing; 2021.
2. Han Y, Bearse MA, Jr, Schneck ME, Barez S, Jacobsen CH, Adams AJ. Multifocal electroretinogram delays predict sites of subsequent diabetic retinopathy. *Invest Ophthalmol Vis Sci.* 2004;45:948–954.
3. Bearse MA, Jr, Han Y, Schneck ME, Adams AJ. Retinal function in normal and diabetic eyes mapped with the slow flash multifocal electroretinogram. *Invest Ophthalmol Vis Sci.* 2004;45:296–304.
4. Lynch SK, Abramoff MD. Diabetic retinopathy is a neurodegenerative disorder. *Vis Res.* 2017;139:101–107.
5. Pardue MT, Barnes CS, Kim MK, et al. Rodent hyperglycemia-induced inner retinal deficits are mirrored in human diabetes. *Transl Vis Sci Technol.* 2014;3:6.
6. Moore-Dotson JM, Beckman JJ, Mazade RE, et al. Early retinal neuronal dysfunction in diabetic mice: reduced light-evoked inhibition increases rod pathway signaling. *Invest Ophthalmol Vis Sci.* 2016;57:1418–1430.
7. Moore-Dotson JM, Eggers ED. Reductions in calcium signaling limit inhibition to diabetic retinal rod bipolar cells. *Invest Ophthalmol Vis Sci.* 2019;60:4063–4073.
8. Castilho A, Ambrosio AF, Hartveit E, Veruki ML. Disruption of a neural microcircuit in the rod pathway of the mammalian retina by diabetes mellitus. *J Neurosci.* 2015;35:5422–5433.
9. Castilho A, Madsen E, Ambrosio AF, Veruki ML, Hartveit E. Diabetic hyperglycemia reduces Ca2+ permeability of extrasynaptic AMPA receptors in AII amacrine cells. *J Neurophysiol.* 2015;114:1545–1553.
10. Ng JS, Bearse MA, Jr, Schneck ME, Barez S, Adams AJ. Local diabetic retinopathy prediction by multifocal ERG delays over 3 years. *Invest Ophthalmol Vis Sci.* 2008;49:1622–1628.
11. Harrison WW, Bearse MA, Jr, Ng JS, et al. Multifocal electroretinograms predict onset of diabetic retinopathy in adult patients with diabetes. *Invest Ophthalmol Vis Sci.* 2011;52:772–777.
12. Fortune B, Schneck ME, Adams AJ. Multifocal electroretinogram delays reveal local retinal dysfunction in early diabetic retinopathy. *Invest Ophthalmol Vis Sci.* 1999;40:2638–2651.
13. Flood MD, Wellington AJ, Cruz LA, Eggers ED. Early diabetes impairs ON sustained ganglion cell light responses and adaptation without cell death or dopamine insensitivity. *Exp Eye Res.* 2020;200:108223.
14. Roy S, Field GD. Dopaminergic modulation of retinal processing from starlight to sunlight. *J Pharmacol Sci.* 2019;140:86–93.
15. Witkovsky P. Dopamine and retinal function. *Doc Ophthalmol.* 2004;108:17–40.
16. Jackson CR, Ruan GX, Aseem F, et al. Retinal dopamine mediates multiple dimensions of light-adapted vision. *J Neurosci.* 2012;32:9359–9368.
17. Mills SL, Xia XB, Hoshi H, et al. Dopaminergic modulation of tracer coupling in a ganglion-amacrine cell network. *Vis Neurosci.* 2007;24:593–608.
18. Perez-Fernandez V, Milosavljevic N, Allen AE, et al. Rod photoreceptor activation alone defines the release of dopamine in the retina. *Curr Biol.* 2019;29:763–774 e765.
19. Farshi P, Fyk-Kolodziej B, Krolewski DM, Walker PD, Ichinose T. Dopamine D1 receptor expression is bipolar cell type-specific in the mouse retina. *J Comp Neurol.* 2016;524:2059–2079.
20. Veruki ML, Wassle H. Immunohistochemical localization of dopamine D1 receptors in rat retina. *Eur J Neurosci.* 1996;8:2286–2297.
21. Cohen AI, Todd RD, Harmon S, O'Malley KL. Photoreceptors of mouse retinas possess D4 receptors coupled to adenylate cyclase. *Proc Natl Acad Sci USA.* 1992;89:12093–12097.
22. Klitten LL, Rath MF, Coon SL, Kim JS, Klein DC, Moller M. Localization and regulation of dopamine receptor D4 expression in the adult and developing rat retina. *Exp Eye Res.* 2008;87:471–477.
23. Li H, Zhang Z, Blackburn MR, Wang SW, Ribelayga CP, O'Brien J. Adenosine and dopamine receptors coregulate photoreceptor coupling via gap junction phosphorylation in mouse retina. *J Neurosci.* 2013;33:3135–3150.
24. Derouiche A, Asan E. The dopamine D2 receptor subfamily in rat retina: ultrastructural immunogold and in situ hybridization studies. *Eur J Neurosci.* 1999;11:1391–1402.
25. Lahouaoui H, Coutanson C, Cooper HM, Bennis M, Dkhissi-Benyahya O. Diabetic retinopathy alters light-induced clock gene expression and dopamine levels in the mouse retina. *Mol Vis.* 2016;22:959–969.
26. Tian T, Li Z, Lu H. Common pathophysiology affecting diabetic retinopathy and Parkinson's disease. *Med Hypotheses.* 2015;85:397–398.
27. Vancura P, Wolloscheck T, Baba K, Tosini G, Iuvone PM, Spessert R. Circadian and dopaminergic regulation of fatty acid oxidation pathway genes in retina and photoreceptor cells. *PLoS One.* 2016;11:e0164665.
28. Kim MK, Aung MH, Mees L, et al. Dopamine deficiency mediates early rod-driven inner retinal dysfunction in diabetic mice. *Invest Ophthalmol Vis Sci.* 2018;59:572–581.
29. Eggers ED, Mazade RE, Klein JS. Inhibition to retinal rod bipolar cells is regulated by light levels. *J Neurophysiol.* 2013;110:153–161.
30. Ivanova E, Toychiev AH, Yee CW, Sagdullaev BT. Optimized protocol for retinal wholemount preparation for imaging and immunohistochemistry. *J Vis Exp.* 2013;e51018.
31. Flood MD, Eggers ED. Dopamine D1 and D4 receptors contribute to light adaptation in ON-sustained retinal ganglion cells. *J Neurophysiol.* 2021;126:2039–2052.

32. Krieger B, Qiao M, Rousso DL, Sanes JR, Meister M. Four alpha ganglion cell types in mouse retina: function, structure, and molecular signatures. *PLoS One*. 2017;12:e0180091.

33. Field GD, Rieke F. Nonlinear signal transfer from mouse rods to bipolar cells and implications for visual sensitivity. *Neuron*. 2002;34:773–785.

34. Andor-Ardo D, Keen EC, Hudspeth AJ, Magnasco MO. Fast, automated implementation of temporally precise blind deconvolution of multiphasic excitatory postsynaptic currents. *PLoS One*. 2012;7:e38198.

35. Nishimura C, Kuriyama K. Alterations in the retinal dopaminergic neuronal system in rats with streptozotocin-induced diabetes. *J Neurochem*. 1985;45:448–455.

36. Aung MH, Park HN, Han MK, et al. Dopamine deficiency contributes to early visual dysfunction in a rodent model of type 1 diabetes. *J Neurosci*. 2014;34:726–736.

37. Vuvan T, Geffard M, Denis P, Simon A, Nguyen-Legros J. Radioimmunoligand characterization and immunohistochemical localization of dopamine D2 receptors on rods in the rat retina. *Brain Res*. 1993;614:57–64.

38. Tran VT, Dickman M. Differential localization of dopamine D1 and D2 receptors in rat retina. *Invest Ophthalmol Vis Sci*. 1992;33:1620–1626.

39. Patel S, Chapman KL, Marston D, Hutson PH, Ragan CI. Pharmacological and functional characterisation of dopamine D4 receptors in the rat retina. *Neuropharmacology*. 2003;44:1038–1046.

40. Jackson CR, Chaurasia SS, Zhou H, Haque R, Storm DR, Iuvone PM. Essential roles of dopamine D4 receptors and the type 1 adenylyl cyclase in photic control of cyclic AMP in photoreceptor cells. *J Neurochem*. 2009;109:148–157.

41. Nir I, Harrison JM, Haque R, et al. Dysfunctional light-evoked regulation of cAMP in photoreceptors and abnormal retinal adaptation in mice lacking dopamine D4 receptors. *J Neurosci*. 2002;22:2063–2073.

42. Pozdeyev N, Tosini G, Li L, et al. Dopamine modulates diurnal and circadian rhythms of protein phosphorylation in photoreceptor cells of mouse retina. *Eur J Neurosci*. 2008;27:2691–2700.

43. Nikolaeva DA, Astakhova LA, Firsov ML. The effects of dopamine and dopamine receptor agonists on the photo-transduction cascade of frog rods. *Mol Vis*. 2019;25:400–414.

44. Sokolov M, Strissel KJ, Leskov IB, Michaud NA, Govardovskii VI, Arshavsky VY. Phosducin facilitates light-driven transducin translocation in rod photoreceptors. Evidence from the phosducin knockout mouse. *J Biol Chem*. 2004;279:19149–19156.

45. Herrmann R, Lobanova ES, Hammond T, et al. Phosducin regulates transmission at the photoreceptor-to-ON-bipolar cell synapse. *J Neurosci*. 2010;30:3239–3253.

46. Ribelayga C, Cao Y, Mangel SC. The circadian clock in the retina controls rod-cone coupling. *Neuron*. 2008;59:790–801.

47. Firsov ML, Astakhova LA. The role of dopamine in controlling retinal photoreceptor function in vertebrates. *Neurosci Behav Physiol*. 2015;46:138–145.

48. Ivanova TN, Alonso-Gomez AL, Iuvone PM. Dopamine D4 receptors regulate intracellular calcium concentration in cultured chicken cone photoreceptor cells: relationship to

49. Snellman J, Kaur T, Shen Y, Nawy S. Regulation of ON bipolar cell activity. *Prog Retin Eye Res*. 2008;27:450–463.

50. Van Hook MJ, Wong KY, Berson DM. Dopaminergic modulation of ganglion-cell photoreceptors in rat. *Eur J Neurosci*. 2012;35:507–518.

51. Ogata G, Stradleigh TW, Partida GJ, Ishida AT. Dopamine and full-field illumination activate D1 and D2-D5-type receptors in adult rat retinal ganglion cells. *J Comp Neurol*. 2012;520:4032–4049.

52. Yin N, Yang YL, Cheng S, et al. Dopamine D2 receptor-mediated modulation of rat retinal ganglion cell excitability. *Neurosci Bull*. 2020;36:230–242.

53. Hwang CK, Chaurasia SS, Jackson CR, Chan GC, Storm DR, Iuvone PM. Circadian rhythm of contrast sensitivity is regulated by a dopamine-neuronal PAS-domain protein 2-adenylyl cyclase 1 signaling pathway in retinal ganglion cells. *J Neurosci*. 2013;33:14989–14997.

54. Dosso AA, Bonvin ER, Morel Y, Golay A, Assal JP, Leuenberger PM. Risk factors associated with contrast sensitivity loss in diabetic patients. *Graefes Arch Clin Exp Ophthalmol*. 1996;234:300–305.

55. Ewing FM, Deary IJ, Strachan MW, Frier BM. Seeing beyond retinopathy in diabetes: electrophysiological and psychophysical abnormalities and alterations in vision. *Endocrine Rev*. 1998;19:462–476.

56. Hyvarinen L, Laurinen P, Rovamo J. Contrast sensitivity in evaluation of visual impairment due to diabetes. *Acta Ophthalmol (Copenh)*. 1983;61:94–101.

57. Di Leo MA, Caputo S, Falsini B, et al. Nonselective loss of contrast sensitivity in visual system testing in early type I diabetes. *Diabetes Care*. 1992;15:620–625.

58. Kunst S, Wolloscheck T, Kelleher DK, et al. Pgc-1alpha and Nr4a1 are target genes of circadian melatonin and dopamine release in murine retina. *Invest Ophthalmol Vis Sci*. 2015;56:6084–6094.

59. Vancura P, Abdelhadi S, Csicsely E, et al. Gnaz couples the circadian and dopaminergic system to G protein-mediated signaling in mouse photoreceptors. *PLoS One*. 2017;12:e0187411.

60. Yujnovsky I, Hirayama J, Doi M, Borrelli E, Sassone-Corsi P. Signaling mediated by the dopamine D2 receptor potentiates circadian regulation by CLOCK:BMAL1. *Proc Natl Acad Sci USA*. 2006;103:6386–6391.

61. Lahouaoui H, Coutanson C, Cooper HM, Bennis M, Dkhissi-Benyahya O. Clock genes and behavioral responses to light are altered in a mouse model of diabetic retinopathy. *PLoS One*. 2014;9:e101584.

62. Qi X, Mitter SK, Yan Y, Busik JV, Grant MB, Boulton ME. Diurnal rhythmicity of autophagy is impaired in the diabetic retina. *Cells*. 2020;9:905.

63. Luo Q, Xiao Y, Alex A, Cummins TR, Bhatwadekar AD. The diurnal rhythm of insulin receptor substrate-1 (IRS-1) and Kir4.1 in diabetes: implications for a clock gene Bmal1. *Invest Ophthalmol Vis Sci*. 2019;60:1928–1936.

64. Motz CT, Chesler KC, Allen RS, et al. Novel detection and restorative levodopa treatment for preclinical diabetic retinopathy. *Diabetes*. 2020;69:1518–1527.